EurJIC
European Journal of Inorganic Chemistry

Full Papers
doi.org/10.1002/ejic.202001072

Chemistry Europe
European Chemical Societies Publishing

VIP *Very Important Paper*

From Missing Links to New Records: A Series of Novel Polychlorine Anions

Patrick Voßnacker,[a] Thomas Keilhack,[a] Nico Schwarze,[a] Karsten Sonnenberg,[a] Konrad Seppelt,[a] Moritz Malischewski,*[a] and Sebastian Riedel*[a]

Herein we report the synthesis and structural characterization of four novel polychloride compounds. The compounds $[CCl(NMe_2)_2][Cl(Cl_2)_3]$ and $[NPr_4][Cl(Cl_2)_4]$ have been obtained from the reaction of the corresponding chloride salts with elemental chlorine at low temperature. They are the missing links in the series of polychloride monoanions $[Cl(Cl)_n]^-$ ($n = 1$–6). Additionally, the reaction of decamethylferrocene with elemental chlorine was studied yielding $[Cp^*_2Fe]_2[Cl_{20}]$, which contains the largest known polychloride $[Cl_{20}]^{2-}$ to date, and $[Cp^*_2Fe][Cl(Cl_2)_4(HF)]$, which is the first example of a polychloride-HF network stabilized by strong hydrogen and halogen bonding. All compounds have been characterized by single-crystal X-ray diffraction, Raman spectroscopy and quantum-chemical calculations.

Introduction

In recent years, polyhalides have received much attention due to various possible applications.[1] They exist as either solids or low viscous ionic liquids with significantly lower vapor pressure compared to the neat halogens.[2] Therefore, trihalides as well as higher polyhalides have been applied as easy-to-handle halogenation reagents which react with ketones,[3] alkenes[4] and alkynes.[3] Additionally, polychlorides have shown to be efficient and safe materials for the storage of elemental chlorine.[5] Recently it was shown that ionic liquids based on polyhalogen- and polyinterhalogen anions can be used for the oxidative dissolution of metals and alloys. Since even noble elements can be dissolved, an application in metal recycling and urban mining might be possible.[6] Besides their potential as oxidation reagents, ionic liquids based on polyhalogen anions possess a surprisingly high conductivity[2] and it was shown that polybromides are present in zinc-bromine (redox flow) batteries.[7]

Polybromides and polyiodides display a structurally rich and diverse chemistry and large anions up to $[Br_{24}]^{2-}$, $[I_{26}]^{4-}$ and $[I_{29}]^{3-}$ can be isolated (Figure 1).[8] In contrast, the more challenging handling of gaseous chlorine as well as the lower stability of polychlorides have so far hampered the exploration of the structural chemistry of polychlorides.[9] Polyfluorides have only been detected under matrix conditions.[10] So far, the only structurally characterized polychlorine monoanions were $[Cl_3]^-$, $[Cl(Cl_2)_2]^-$[11] and only very recently crystal structures of $[Cl(Cl_2)_5]^-$ and $[Cl(Cl_2)_6]^-$ were reported.[12] The $[Cl_3]^-$ anion possesses a nearly linear structure in the solid state while the structure of the $[Cl(Cl_2)_2]^-$ within $[PPh_2Cl_2][Cl(Cl_2)_2]]$ ($[PPh_2Cl_2]^+$ = diphenyldichlorophosphonium) can best be described as a hockey stick structure.[1,11b] $[Cl(Cl_2)_5]^-$ exists as either isolated square pyramidal structure ($[PPN][Cl(Cl_2)_5]\cdot Cl_2$, $[PPN]^+$ = bis(triphenylphosphine)iminium) or as square pyramidal $[Cl(Cl_2)_5]^-$ unit which are connected by one Cl_2 molecule (octahedral coordination for the central halide) forming infinite chains ($[PPh_4][Cl(Cl_2)_5]$, $[AsPh_4][Cl(Cl_2)_5]$; $[PPh_4]^+$ = tetraphenylphosphonium, $[AsPh_4]^+$ = tetraphenylarsonium). The polychloride with

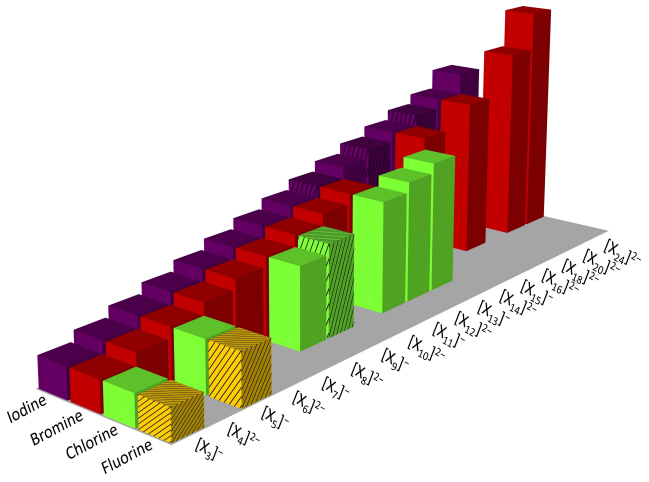

Figure 1. Overview of experimentally known homoatomic polyhalogen mono- and dianions. These anions have been crystallographically characterized except for the shaded ones, which have only been observed spectroscopically. Reproduced from ref.[1]

[a] *P. Voßnacker, T. Keilhack, Dr. N. Schwarze, Dr. K. Sonnenberg, Prof. Dr. K. Seppelt, Dr. M. Malischewski, Prof. Dr. S. Riedel*
Fachbereich Biologie, Chemie, Pharmazie
Institut für Chemie und Biochemie – Anorganische Chemie
Fabeckstr. 34/36, 14195 Berlin, Germany
E-mail: moritz.malischewski@fu-berlin.de
s.riedel@fu-berlin.de
https://www.bcp.fu-berlin.de/chemie/chemie/forschung/InorgChem/ag-malischewski
www.fluorinechemistry.de

Supporting information for this article is available on the WWW under https://doi.org/10.1002/ejic.202001072

Part of the joint "German Chemical Society ADUC Prizewinner" Collection with EurJOC.

the highest chlorine content, $[Cl(Cl_2)_6]^-$, has an octahedral geometry in the solid state.[12] So far, only two polychlorine dianions are known in the literature. The $[Cl_8]^{2-}$ ($[CCl(NMe)_2]_2[Cl_8]$[13], $[CCl(NMe)_2]^+$ = tetramethylchloroamidinium) which shows a discrete, Z-shaped structure and the $[Cl_{12}]^{2-}$ ($[NMe_3Ph]_2[Cl_{12}]$[12], $[NMe_3Ph]^+$ = trimethylphenylammonium) which possesses inversion symmetry and can be described as two $[Cl(Cl_2)_2]^-$ units which are connected by a Cl_2 molecule. The $[Cl_{12}]^{2-}$ units are further connected to form a three-dimensional network resembling a honeycomb. In 2015 the molecular structure of a 2D layered infinite polychlorine structure consisting of $[Cl_3]^-$ and Cl_2 building blocks ($[NEt_4][Cl_3)_2 \cdot Cl_2]$, $[NEt_4]^+$ = tetraethylammonium) was described.[14]

The bonding situation of such higher polyhalogen anions can be described as a Lewis acid-base interaction between the halide (Lewis base) and the dihalogen (Lewis acid). Two major interactions contribute to the bonding: First there is charge transfer from the HOMO of the halide ion (lone pair) into the LUMO of the dihalogen (σ*(X–X)) which leads to an elongation of the X–X bond. Additionally, the electrostatic potential of the dihalogen is anisotropic. This results in a belt of higher electron density perpendicular to the molecule's bonding axis and an area of lower electron density along the extension of the covalent bond, the so called σ-hole. Between the negatively charged halide ion and the positive σ-hole there is an attractive electrostatic interaction.[15] Very recently the bonding situation of the $[Cl_3]^-$ has been studied by experimental and computed electron densities determination. It was shown that a genuine ppσ bond is formed if a chlorine molecule interacts with a "naked" chloride ion. Furthermore, it appears to be a smooth transition from the asymmetric to the symmetric compound which is a crucial property for its chemical reactivity.[16]

Herein, we report the synthesis and characterization of four hitherto unknown polychloride compounds. It was possible to obtain the first molecular structures of a heptachloride ($[CCl(NMe_2)_2][Cl(Cl_2)_3]$) and a nonachloride ($[NPr_4][Cl(Cl_2)_4]$). In addition, the first polychloride-HF network was synthesized ($[Cp^*_2Fe]_2[Cl(Cl_2)_4(HF)]$) and the largest known polychloride, the $[Cl_{20}]^{2-}$ could be obtained by oxidation of Cp^*_2Fe with a large excess of chlorine.

Results and Discussion

The Heptachloride $[Cl(Cl_2)_3]^-$

An anion, which can formally be described as a $[Cl(Cl_2)_3]^-$, was obtained by the reaction of the Vilsmeier salt $[CCl(NMe_2)_2]Cl$ with a large excess of chlorine without additional solvent (Equation 1).

$$[CCl(NMe_2)_2]Cl + 3Cl_2 \xrightarrow[25^\circ C \rightarrow -40^\circ C]{Cl_2} [CCl(NMe_2)_2][Cl(Cl_2)_3] \downarrow \quad (1)$$

By slowly cooling the reaction mixture to −40 °C single crystals of $[CCl(NMe_2)_2][Cl(Cl_2)_3]$ were obtained which crystalize in the orthorhombic space group $P2_12_12_1$ (Figure 2).

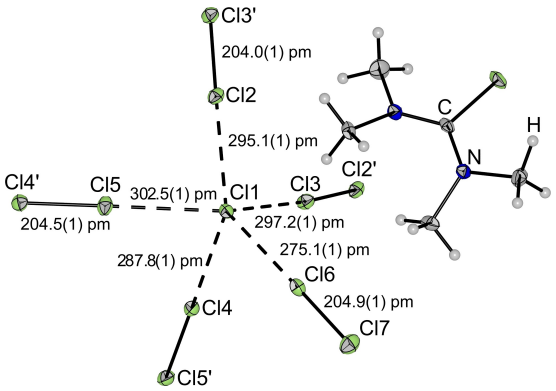

Figure 2. Molecular structure of $[CCl(NMe_2)_2][Cl(Cl_2)_3]$ in the solid state with thermal ellipsoids shown at 50 % probability.

The anion within $[CCl(NMe_2)_2][Cl(Cl_2)_3]$ is best described as a polychloride network in which the central chloride is coordinated by five chlorine molecules, four of them are bridging to the next chloride ion while one is terminal. Four chloride ions connected by four chlorine molecules form a bent rectangle, with the fifth chlorine alternatingly pointing up and downwards. The bent rectangles are connected by all four edges to form an extended network (Figure 3).

The distance between the central halide and the terminal Cl_2 unit (275.1(1) pm) as well as the Cl_2 bond length (204.9(1) pm) are in good agreement to the bond length calculated on SCS-MP2/def2-TZVPP for a square pyramidal $[Cl(Cl)_5]^-$ anion (277.8–282.2 pm, 203.9–204.8 pm). In comparison to crystalline Cl_2 (R(Cl–Cl) = 198.4(1) pm) the Cl_2 bond length is elongated by 6.5(2) pm which can be explained by the aforementioned donation of electron density into the σ*-orbital of the Cl–Cl bond which leads to a bond weakening effect. The distance between the central halide and the bridging Cl_2 units is significantly longer (287.8(1)–302.5(1) pm). Nevertheless, the

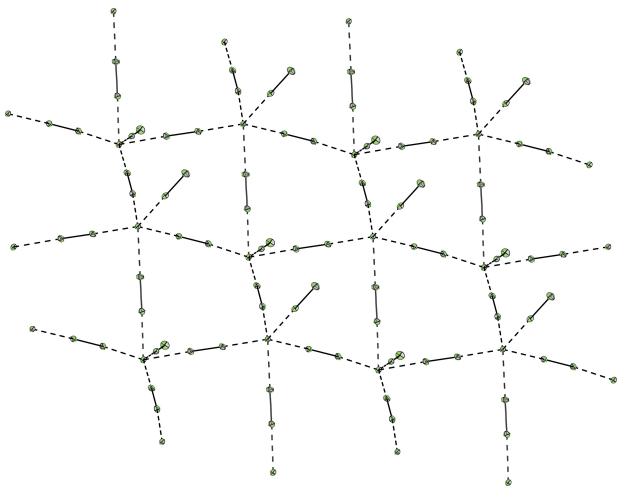

Figure 3. Structure of the polychlorine monoanion within the solid state structure of $[CCl(NMe_2)_2][Cl(Cl_2)_3]$. Thermal ellipsoids are shown at 50 % probability. Cations are omitted for clarity.

weakening of the Cl–Cl bond is comparable for the bridging Cl_2 units (R(Cl–Cl) = 204.0(1)–204.5 pm) which is due to a charge transfer from two chloride ions. The shortest distances between cation and anion are a Cl–H distance of 274.0(3) pm and a Cl–Cl distance of 339.1(1) pm which indicate moderate hydrogen and halogen bonding interactions.

The Raman spectrum of the single crystal of $[CCl(NMe_2)_2]_2[Cl(Cl_2)_3]$ shows three bands at 471, 451 and 430 cm^{-1} (see Figure S8). Those bands correspond to the stretching modes of the three crystallographic independent Cl_2 units in the crystal. The experimentally obtained spectra is rather similar to the computed spectra at SCS-MP2/def2-TZVPP level for a C_{4v} symmetric $[Cl(Cl_2)_5]^-$ anion in the gas phase while no exact match can be expected due to the network structure in the solid state (see Figure S9).

The Nonachloride $[Cl(Cl_2)_4]^-$

$[NPr_4][Cl(Cl_2)_4]$ ($[NPr_4]^+$ = tetrapropylammonium) was prepared by condensing stoichiometric amounts of chlorine onto an acetonitrile (MeCN) solution of $[NPr_4]Cl$ (Equation 2).

$$[NPr_4]Cl + 4Cl_2 \xrightarrow[25^\circ C \rightarrow -15^\circ C]{MeCN} [NPr_4][Cl(Cl_2)_4] \downarrow \quad (2)$$

By slowly cooling to −15 °C single crystals of $[NPr_4][Cl(Cl_2)_4]$ were obtained which crystalize in the tetragonal space group $I\bar{4}$. (Figure 4). The structure of the anion can best be described as a distorted tetrahedron. Quantum-chemical calculations (B3LYP(D3BJ)/def2-TZVPP and SCS-MP2/def2-TZVPP (value in parentheses) predicted the tetrahedral structure to be the minimum in the gas phase. In comparison the pyramidal structure (C_{4v}) is 8.54 (4.29) kJ mol^{-1} higher in energy and shows one imaginary frequency (transition state between two tetrahedral structures) while the planar structure (D_{4h}) is 9.7 (4.4) kJ mol^{-1} higher in energy and shows one (MP2) or two (B3LYP) imaginary frequencies (transition between tetrahedral as well as pyramidal structures). The bond length of the coordinated Cl_2 is elongated by 8.1(6) pm when compared to crystalline Cl_2 (R(Cl–Cl) = 198.4(1) pm)[17] which agrees well with the computed bond length on MP2 level of theory (R(Cl–Cl) = 205.6 pm). In the Raman spectrum of the single crystal two bands at 477 and 450 are observed in the Cl_2 region. Those bands are in good agreement to the calculated bands on SCS-MP2 level at 472 and 438 cm^{-1} (Figure S9).

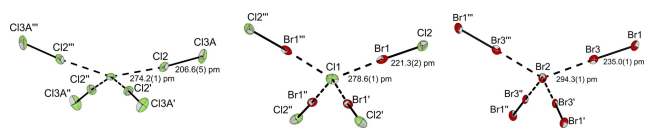

Figure 4. Comparison of the molecular structure of $[NPr_4][Cl(Cl_2)_4]$, $[NPr_4][Cl(BrCl)_4]$ and $[NPr_4][Br(Br_2)_4]$ in the solid state. Thermal ellipsoids are shown at 50% probability. Disorders are omitted for clarity (see Figure S2 for structure including disorder). Bond angles in [°]: Cl2–Cl1–Cl2′ 93.2(1), Cl2–Cl1–Cl2‴ 152.6(1), Br1–Cl1–Br1′ 100.3(1), Br1–Cl1–Br1‴ 130.1(1), Br3–Br2–Br3′ 99.8(1), Br3–Br2–Br3‴ 131.2(1).

Two isostructural compounds, $[NPr_4][Cl(BrCl)_4]$[18] and $[NPr_4][Br(Br_2)_4]$[19], are known in the literature. When the structures of the polyhalogen anions are compared it can be seen that the distortion of the tetrahedra is most pronounced for the $[Cl(Cl)_4]^-$ anion (bond angles of 93.2(1)° and 152.6(1)°, compared to 100.3(1)°, 130.1(1)° for $[Cl(BrCl)_4]^-$ and 99.8(1)°, 131.2(1)° for $[Br(Br_2)_4]^-$). This can be explained by inter-molecular interactions. Within the molecular structure of $[NPr_4][Br(Br_2)_4]$ there are short Br3–Br1 distances of 339.5(1) pm ($\Sigma_{vdW\,radii}$ = 370 pm)[20] yielding a connection between the $[Br(Br_2)_4]^-$ units by forming eight-membered folded rectangles (see Figure 5B). When going from Br_2 to BrCl the structure of the anion does not change much but the inter-molecular interactions get weaker (Br1–Cl2 distances of 350.8(2) pm, $\Sigma_{vdW\,radii}$ = 360 pm[20]) due to the shorter Br–Cl bonds which increases the distance between the $[Cl(BrCl)_4]^-$ units (see Figure S4). Due to the even shorter Cl–Cl bond lengths the distances between the $[Cl(Cl_2)_4]^-$ units would become so large that there would be no inter-molecular interactions. Therefore, for the $[Cl(Cl_2)_4]^-$ unit, a stronger distortion is observed which allows inter-molecular interaction by short Cl3A–Cl3A distances of 319(1) pm ($\Sigma_{vdW\,radii}$ = 350 pm)[20] forming four-membered folded rectangles (see Figure 5A).

Reactions of $[Cp^*_2Fe]$ with Cl_2

The reactions of ferrocene with dihalogens are known for a long time.[21] Ferrocenium is well known to form a series of polyiodide complexes, from the triiodide $[Cp_2Fe][I_3]$[21], $[Cp_2Fe][I_7]$[22], $[Cp_2Fe]_2[I_{16}]$[23] to $[Cp_2Fe]_3[I_{29}]$[8c] (Cp_2Fe = ferrocene, Cp^*_2Fe = decamethylferrocene). However, elemental bromine or chlorine are so reactive, that they partially or completely destroy the ferrocene moiety, leading to either $[Cp_2Fe][FeX_4]$ or pentahalocyclopentane $C_5H_5X_5$ (X=Cl, Br).[24] Only a small number of ferrocenium derivatives with tribromide counter anions have been isolated so far.[25]

Recently it was shown that ferrocene derivatives can be oxidized twice to form stable compounds containing tetravalent iron ($[Cp^*_2Fe]^{2+}$, $[Cp^*_2FeCO]^{2+}$ and $[Cp_2FeH^+]$).[26] Therefore it was attempted to oxidize $[Cp^*_2Fe]$ using an excess of the strong oxidizer Cl_2 to form either $[Cp^*_2Fe]^{2+}$ or the unknown

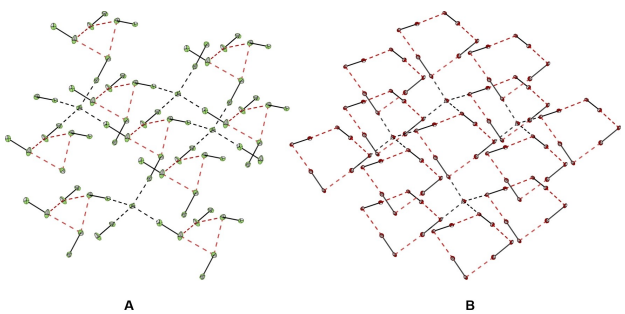

Figure 5. Anion network within the solid state structures of $[NPr_4][Cl(Cl_2)_4]$ (A) and $[NPr_4][Br(Br_2)_4]$ (B). Intermolecular interactions are indicated by red dotted lines.

$[Cp^*_2FeCl]^+$. Although oxidation to $[Cp^*_2Fe]^+$ occurs rapidly in dichloromethane, longer reaction times at room temperature (especially in the sunlight) lead to chlorination or cleavage of the Cp* ligand. A two-electron oxidation of the $[Cp^*_2Fe]$ was not observed. Slowly cooling the reaction mixture to −75 °C yields green single crystals of $[Cp^*_2Fe][Cl(Cl_2)_4(HF)]$ (Equation 3).

$$[Cp^*_2Fe] + 4.5Cl_2 + HF \xrightarrow[-35^\circ C \rightarrow -75^\circ C]{DCM} [Cp^*_2Fe][Cl(Cl_2)_4(HF)] \downarrow \quad (3)$$

Co-crystalized HF is most likely a result of adventitious traces of HF which were present since the reaction was performed in a PFA reactor on a steel line which was previously used for reactions involving HF. To rule out a contamination with water (differentiation between HF and H_2O is not always possible by XRD) the reaction was repeated, and stoichiometric amounts of HF and H_2O were added, respectively. The addition of milligram amounts of HF led to the formation of the same crystals, while addition of water was inconclusive.

$[Cp^*_2Fe][Cl(Cl_2)_4(HF)]$ crystalizes in the monoclinic space group *C*2/*m* (Figure 6).

The structure of the anion can be described as an intermediate between a square pyramidal structure with HF on the top of the pyramid (C_{4v}) and a trigonal bipyramidal (C_{2v}) structure with HF in an equatorial position. This interpretation is further supported by the structural parameter τ which was calculated to be 0.56 (τ = (β-α/60°, α and β are the largest angle in the coordination sphere; τ = 0 for perfect square-pyramidal structure and 1 for perfect bipyramidal symmetric structure)[27]. Quantum-chemical calculations in the gas-phase predict both structures to be very close in energy. On B3LYP(D3BJ)/def2-TZVPP level of theory the C_{2v} structure is favored by 0.5 kJ mol^{-1} with the C_{4v} being a transition state while on SCS-MP2 level of theory the C_{4v} symmetric structure is equal in energy both being minima, indicating a very shallow potential energy surface. The bond length of the coordinated Cl_2 is only slightly elongated by 2.7(2) to 4.3(2) pm when compared to crystalline Cl_2 (*R*(Cl–Cl) = 198.4(1) pm)[17] while the short F1–Cl1 distance of 289.1(2) pm indicate strong hydrogen bonding interaction. A comparison with the molecular structure of $[PPN][Cl(Cl_2)_5]\cdot Cl_2$, in which the central chloride also has a coordination number of five, shows a comparable weakening of the Cl–Cl bond with bond length of 201.5(1) to 202.6(1) pm.[12] This indicates that the Lewis acidity of the HF molecule is at least comparable to the Lewis acidity of Cl_2. Quantum-chemical calculations support this observation since the addition of a HF molecule to $[Cl(Cl_2)_4]^-$ was calculated (B3LYP(D3BJ)/def2-TZVPP and SCS-MP2/def2-TZVPP (value in parentheses) to be 8.6 (13.3) kJ mol^{-1} exergonic while the exchange of one Cl_2 unit from $[Cl(Cl_2)_5]^-$ against one HF molecule is 17.2 (32.0) kJ mol^{-1} exergonic (Scheme 1).

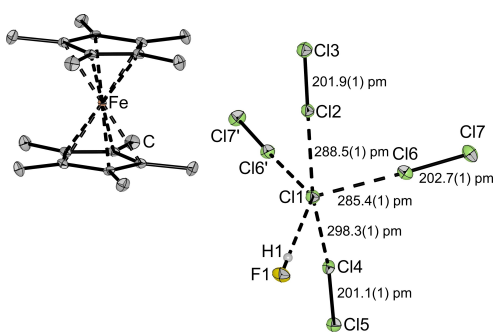

Figure 6. Molecular structure of $[Cp^*_2Fe][Cl(Cl_2)_4(HF)]$ in the solid state with thermal ellipsoids shown at 50% probability. The F1–Cl1 distance is 289.1(2) pm. Hydrogen atoms are omitted for clarity.

This also explains why a mixed anion containing HF and Cl_2 is obtained even when an excess of chlorine was used. Further quantum-chemical calculations show that in principle all exchange reactions of Cl_2 against HF are exergonic for the system $[Cl(Cl_2)_{5-n}(HF)_n] + HF \rightarrow [Cl(Cl_2)_{5-n-1}(HF)_{n+1}]^- + Cl_2$ (n = 0–4, see Table S6) while an exchange of Cl_2 in $[Cl(Cl_2)_5]^-$ against HCl is also exergonic (Table S7).

The Raman spectrum of the single crystal of $[Cp^*_2Fe][Cl(Cl_2)_4(HF)]$ shows three bands at 507, 488 and 477 cm^{-1}. Those bands agree well to the bands calculated on SCS-MP2/def2-TZVPP level of theory for a C_{2v} symmetric $[Cl(Cl_2)_4(HF)]^-$ (499, 480, 477 cm^{-1}) while again no exact match can be expected due to the reduced symmetry in the crystal and the formation of the polyhalide network (see Figure S9).

When an even larger excess of Cl_2 (21 equiv.) is used in absence of HF slow cooling of the reaction mixture to −75 °C yields single crystals of $[Cp^*_2Fe]_2[Cl_{20}]$ which represents the largest known polychloride today. (Equation 4).

$$2[Cp^*_2Fe] + 10Cl_2 \xrightarrow[-50^\circ C \rightarrow -75^\circ C]{DCM/Cl_2} [FeCp^*_2]_2[Cl_{20}] \downarrow \quad (4)$$

$[Cp^*_2Fe]_2[Cl_{20}]$ crystallizes in the monoclinic space group *C*2/*c* (Figure 7).

The structure of the anion is interpreted as two $[Cl(Cl_2)_4]^-$ units which are connected by a single bridging Cl_2 molecule. Overall, the structure of the anion is rather asymmetric with large differences in the distance between the central halide and the coordinated Cl_2 unit (*R*(Cl–Cl) = 271.4(1) to 299.2(1) pm). This might be due to further inter-molecular interactions to other $[Cl_{20}]^{2-}$ units. The Cl_2 bond length of the coordinated Cl_2 units correlates well to the distance to the central halide. It increases when the distance is shorter which can be explained by a stronger interaction and therefore more donation of electron density into the σ* orbital of the Cl–Cl bond. The only exception is the bridging Cl_2 which has a significantly elongated bond (203.6(1) pm) even though the distance to the chloride ion is rather large (299.2(1) pm). This is due to the interaction with two Cl^- ions. The Raman spectrum shows five bands between 490 and 419 cm^{-1} (see Figure S8). This is in agreement with the symmetry of the anion as the $[Cl_{20}]^{2-}$ exhibits inversion

$$[Cl(Cl_2)_4]^- + HF \xrightarrow{\Delta G = -8.6\ (-13.3)\ kJ\ mol^{-1}} [Cl(Cl_2)_4(HF)]^-$$

$$[Cl(Cl_2)_5]^- + HF \xrightarrow{\Delta G = -17.2\ (-32.0)\ kJ\ mol^{-1}} [Cl(Cl_2)_4(HF)]^- + Cl_2$$

Scheme 1. Free reaction energies for the reaction of $[Cl(Cl_2)_4]^-$ with HF and for the substitution of one Cl_2 against one HF in $[Cl(Cl_2)_5]^-$.

Full Papers
doi.org/10.1002/ejic.202001072

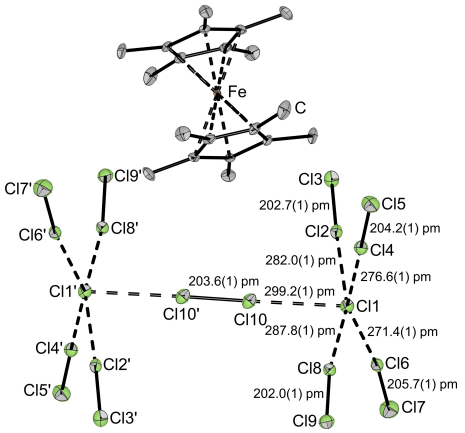

Figure 7. Molecular structure of $[Cp^*_2Fe]_2[Cl_{20}]$ in the solid state with thermal ellipsoids shown at 50% probability. Only one cation and no hydrogen atoms are shown for clarity.

symmetry (C_i). Therefore, the rule of mutual exclusion holds, and only vibrations of *g* symmetry are visible in the Raman spectrum. For a C_i symmetric $[Cl_{20}]^{2-}$, five bands with A_g symmetry are computed on B3LYP(D3BJ)-COSMO/def2-TZVPP and SCS-MP2-COSMO/def2-TZVPP ($\varepsilon_{rel} = 100$) level of theory (see Figure S9). The broad area of wavenumbers over which the bands are spread can be explained by the rather large differences in the Cl–Cl bond length (R(Cl–Cl) = 202.0(1)–205.7(1) pm).

Both the $[Cl(Cl_2)_4(HF)]^-$ and the $[Cl_{20}]^{2-}$ form three-dimensional networks in the solid state. The $[Cl(Cl_2)_4(HF)]^-$ forms hexagonal prisms via short inter-molecular F–Cl distances of F1–Cl3 273.9(2) pm, F1–Cl5 287.8(2) pm and F1–Cl7 283.2(2) pm ($\Sigma_{vdW\,radii} = 322$ pm[20], see Figure 8). This gives a coordination number of five for the central chloride as well as for the fluorine of the HF molecule. In this case the fluorine acts as a halogen bond acceptor (Lewis base) to connect the $[Cl(Cl_2)_4(HF)]^-$ units. The center of the hexagonal prism is occupied by a $[Cp^*_2Fe]^+$ cation with the prisms being connected via all eight phases to translate in all three dimensions (see Figure S5.) For the $[Cl_{20}]^{2-}$ the same hexagonal prismatic arrangement is observed in the solid state, even though the prism is heavily distorted (See Figure 8). The Hirshfeld surface of the $[Cl_{20}]^{2-}$ unit shows significant interactions between the anions while only weak interactions with the cations are observed (See Figure S7). Nevertheless, a description as discrete $[Cl_{20}]^{2-}$ units is reasonable since the inter-molecular distances of R(Cl6–Cl3) = 326.9(1) pm, R(Cl6–Cl5) = 336.9(1) pm, R(Cl6–Cl9) = 324.8(1) pm and R(Cl7–Cl7) = 321.8(2) pm ($\Sigma_{vdW\,radii} = 350$ pm)[20] are significantly longer than the longest intramolecular distance (at least 22.6 pm).

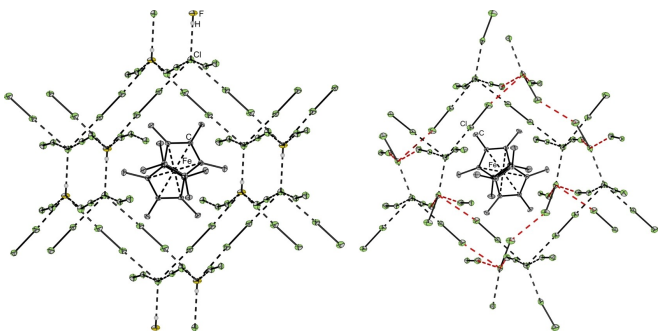

Figure 8. Anion network within the solid state structure of $[Cp^*_2Fe][Cl(Cl_2)_4(HF)]$ and $[Cp^*_2Fe]_2[Cl_{20}]$. Thermal ellipsoids are shown at 50% probability. Hydrogen atoms are omitted for clarity. Intramolecular interactions between the $[Cl_{20}]^{2-}$ units are indicated by red dotted lines.

Conclusion

In this work the synthesis of the four hitherto unknown polychlorides compounds, $[CCl(NMe_2)_2][Cl(Cl_2)_3]$, $[NPr_4][Cl(Cl_2)_4]$, $[Cp^*_2Fe][Cl(Cl_2)_4(HF)]$ and $[Cp^*_2Fe]_2[Cl_{20}]$ was reported. All compounds have been thoroughly characterized by single-crystal X-ray diffraction, single crystal Raman spectroscopy as well as quantum-chemical calculations. With the syntheses of $[Cl(Cl)_3]^-$ and $[Cl(Cl)_4]^-$ the row of polychloride monoanions $[Cl(Cl_2)_n)]^-$ ($n = 1$–6) was completed while with $[Cp^*_2Fe]_2[Cl_{20}]$ we succeeded in the synthesis of the largest known polychloride. Additionally, the $[Cl(Cl_2)_4(HF)]^-$ anion is the first example for a polychloride-HF network which is stabilized by strong hydrogen and halogen bonding interaction. Overall, it could be shown that polychloride chemistry shows a surprising structural diversity, which is comparable to that of the heavier polyhalogen anions.

Experimental Section

Apparatus and Materials

All substances sensitive to water and oxygen were handled under an argon atmosphere using standard Schlenk techniques and oil pump vacuum up to 10^{-3} mbar. Some reactions were performed on a stainless steel vacuum line in self-built reactors consisting of 8 mm o. d. PFA (perfluoroalkoxy alkanes) tubing which where heat sealed on one end and connected to a steel valve on the other end. Dry DCM was obtained by storage over activated 3 Å molecular sieves. Commercially available $[NPr_4]Cl$ and Cp^*_2Fe were used without further purification. Chlorine (Linde, purity 2.8) was passed through calcium chloride to remove traces of water. $[CCl(NMe_2)_2]Cl$[28] was prepared according to literature procedures. All salts were dried *in vacuo* at 100 °C for 10 min prior to use. Raman spectra were recorded on a Bruker (Karlsruhe, Germany) MultiRAM II equipped with a low-temperature Ge detector (1064 nm, 100–180 mW, resolution of 4 cm^{-1}). Spectra of single crystals were recorded at −196 °C using the Bruker RamanScope III (see supporting information part g for description of the used method). X-ray diffraction data were collected on a Bruker D8 Venture CMOS area detector (Photon 100) diffractometer with $Mo_{K\alpha}$ radiation. Single crystals were coated with perfluoroether oil at low temperature (−40/−80 °C) and mounted on a 0.1–0.2 mm Micromount. The structures were solved with the ShelXT[29] structure solution program using intrinsic phasing and refined with the ShelXL[30] refinement package using least squares on weighted F2

values for all reflections using OLEX2[31]. For quantum chemical calculations (structure optimization (with and without solvent model COSMO[32]) and frequency calculations (including Raman intensities)) the program package TURBOMOLE 7.3[33] was used. Functionals (B3LYP(D3BJ)[34] and SCS-MP2[35]) and the basis set (def2-TZVPP)[36] were used as implemented in TURBOMOLE. Minima on the potential energy surface were characterized by harmonic vibrational frequency analysis. Thermochemistry was provided with zero-point vibration correction, ΔG values were calculated at 298.15 K and 1.0 bar. Representations of Hirshfeld surfaces were generated using CrystalExplorer17[37]

$[CCl(NMe_2)_2][Cl(Cl_2)_3]$

1.57 g (22.45 mmol, 15.4 equiv.) Cl_2 were condensed onto 250 mg (1.46 mmol) $[CCl(NMe_2)_2]Cl$ at −196 °C. Warming to room temperature yields a clear yellow solution. Yellow single crystals of $[CCl(NMe_2)_2][Cl(Cl_2)_3]$ were obtained within several days by slowly cooling to −40 °C.

$[CCl(NMe_2)_2][Cl(Cl_2)_3]$ Raman (−196 °C): $\tilde{\nu}$ = 2950 (vw), 2985 (vw), 1456 (vw), 1389 (vw), 618 (vw), 471 (vs), 451 (vs), 430 (m), 272 (m), 146 cm^{-1} (vw).

CCDC number: 2031714

$[NPr_4][Cl(Cl_2)_4]$

601 mg (2.7 mmol) $[NPr_4]Cl$ was dissolved in 1.4 mL MeCN. 766 mg (10.9 mmol, 4.0 equiv.) Cl_2 are condensed onto the solution at −196 °C. The reaction mixture was warmed to room temperature and a clear yellow solution was obtained. Yellow single crystals of $[NPr_4][Cl(Cl_2)_4]$ were obtained within several days by slowly cooling to −15 °C.

$[NPr_4][Cl(Cl_2)_4]$ Raman (−196 °C): $\tilde{\nu}$ = 3003 (vw), 2982 (vw), 2954 (vw), 2937 (vw), 2872 (vw), 1458 (vw), 1445 (vw), 1315 (vw), 477 (vs), 450 (vs), 151 cm^{-1}(w).

CCDC number: 2031713

$[Cp^*_2Fe][Cl(Cl_2)_4(HF)]$

Inside a 8 mm PFA tube connected to a stainless steel valve, 32 mg (0.1 mmol) Cp^*_2Fe were dissolved in 1.5 ml dichloromethane. 90 mg Cl_2 (1.25 mmol) were condensed in at −196 °C. The mixture was warmed to −70 °C and mechanically agitated resulting in a dark green suspension. After some minutes 3 mg anhydrous hydrogen fluoride were condensed in at −196 °C. The mixture was warmed to approximately −35 °C, resulting in a clear dark-green solution. The mixture was frozen at −196 °C, and the PFA tube was flame-sealed in vacuum. The sealed-off tube was placed inside a Dewar filled with 1–2 liters of −35 °C cold ethanol and placed in a −75 °C freezer. After one day, dark-green crystals had formed.

$[Cp^*_2Fe][Cl(Cl_2)_4(HF)]$ Raman (−196 °C): $\tilde{\nu}$ = 2931 (m), 1423 (w), 735 (w), 588 (w), 507 (s), 488 (s), 477 (vs), 367 (w), 292 (vw).

CCDC number: 2031710

$[Cp^*_2Fe]_2[Cl_{20}]$

Inside a 8 mm PFA tube connected to a stainless steel valve, 32 mg (0.1 mmol) Cp^*_2Fe were dissolved in 1.5 ml dichloromethane. 180 mg Cl_2 (2.5 mmol) were condensed in at −196 °C. The mixture was warmed to −70 °C and mechanically agitated resulting in a dark green suspension. After some minutes, the mixture was warmed to −50 °C, resulting in a clear dark-green solution. The mixture was frozen at −196 °C, and the PFA tube was flame-sealed in vacuum. The sealed-off tube was placed inside a Dewar filled with 1–2 liters of −50 °C cold ethanol and placed in a −75 °C freezer. After one day, dark-green crystals had formed.

$[Cp^*_2Fe]_2[Cl_{20}]$ Raman (−196 °C): $\tilde{\nu}$ = 2986 (vw), 2965 (vw), 2914 (w), 1480 (vw), 1442 (vw), 1425 (vw), 1025 (vw), 700 (vw), 591 (vw), 490 (s), 473 (vs), 450 (vs), 417 (m), 366 (w), 291 (m), 242 (vw), 223 (vw), 182 cm^{-1} (vw).

CCDC number: 2031711.

Deposition Numbers 2031714 (for $[CCl(NMe_2)_2][Cl(Cl_2)_3]$), 2031713 (for $[NPr_4][Cl(Cl_2)_4]$), 2031710 (for $[Cp^*_2Fe][Cl(Cl_2)_4(HF)]$), and 2031711 (for $[Cp^*_2Fe]_2[Cl_{20}]$) contain the supplementary crystallographic data for this paper. These data are provided free of charge by the joint Cambridge Crystallographic Data Centre and Fachinformationszentrum Karlsruhe Access Structures service www.ccdc.cam.ac.uk/structures.

Acknowledgements

We gratefully acknowledge the Zentraleinrichtung für Datenverarbeitung (ZEDAT) of the FU Berlin for computational resources. We thank the priority program SPP 1708 for financial support. We thank Tyler Andrew Gully for helping prepare the table of contents graphic. Open access funding enabled and organized by Projekt DEAL.

Conflict of Interest

The authors declare no conflict of interest.

Keywords: Halogens · Polychlorides · Quantum-chemical calculations · Halogen-bonding · Structure elucidation

[1] K. Sonnenberg, L. Mann, F. A. Redeker, B. Schmidt, S. Riedel, *Angew. Chem. Int. Ed.* **2020**, *59*, 5464–5493, *Angew. Chem.* **2020**, *132*, 5506–5535.
[2] H. Haller, M. Hog, F. Scholz, H. Scherer, I. Krossing, S. Riedel, *Z. Naturforsch.* **2013**, *68b*, 1103–1107.
[3] T. Schlama, K. Gabriel, V. Gouverneur, C. Mioskowski, *Angew. Chem. Int. Ed.* **1997**, *36*, 2342–2344, *Angew. Chem.* **1997**, *109*, 2440–2442.
[4] a) T. M. Beck, H. Haller, J. Streuff, S. Riedel, *Synthesis* **2014**, *46*, 740–747; b) S. S. Tartakoff, C. D. Vanderwal, *Org. Lett.* **2014**, *16*, 1458–1461; c) C. V. Vogel, H. Pietraszkiewicz, O. M. Sabry, W. H. Gerwick, F. A. Valeriote, C. D. Vanderwal, *Angew. Chem. Int. Ed.* **2014**, *53*, 12205–12209, *Angew. Chem.* **2014**, *126*, 12401–12405; d) W.-j. Chung, J. S. Carlson, C. D. Vanderwal, *J. Org. Chem.* **2014**, *79*, 2226–2241; e) Z. A. Könst, A. R. Szklarski, S. Pellegrino, S. E. Michalak, M. Meyer, C. Zanette, R. Cencic, S. Nam, V. K. Voora, D. A. Horne, J. Pelletier, D. L. Mobley, G. Yusupova, M. Yusupov, C. D. Vanderwal, *Nat. Chem.* **2017**, *9*, 1140–1149.
[5] a) M. Paven, Y. Schiesser, R. Weber, G. Langstein, V. Trieu, S. Riedel, N. Schwarze, S. Steinhauer, **2018**, WO 2019215037 A1; b) A. N. Usoltsev, S. A. Adonin, B. A. Kolesov, A. S. Novikov, V. P. Fedin, M. N. Sokolov, *Chem. Eur. J.* **2020**, *26*, 13776–13778.
[6] a) A. van den Bossche, E. de Witte, W. Dehaen, K. Binnemans, *Green Chem.* **2018**, *20*, 3327–3338; b) X. Li, A. van den Bossche, T. Vander Hoogerstraete, K. Binnemans, *Chem. Commun.* **2018**, *54*, 475–478; c) X. Li, Z. Li, M. Orefice, K. Binnemans, *ACS Sustainable Chem. Eng.* **2019**, *7*, 2578–2584; d) B. Schmidt, B. Schröder, K. Sonnenberg, S. Steinhauer, S. Riedel,

Angew. Chem. Int. Ed. **2019**, *58*, 10340–10344, *Angew. Chem.* **2019**, *131*, 10448.
[7] G. Bauer, J. Drobits, C. Fabjan, H. Mikosch, P. Schuster, *J. Electroanal. Chem.* **1997**, *427*, 123–128.
[8] a) M. E. Easton, A. J. Ward, T. Hudson, P. Turner, A. F. Masters, T. Maschmeyer, *Chem. Eur. J.* **2015**, *21*, 2961–2965; b) K.-F. Tebbe, R. Buchem, *Z. Anorg. Allg. Chem.* **1998**, *624*, 671–678; c) K.-F. Tebbe, R. Buchem, *Angew. Chem. Int. Ed. Engl.* **1997**, *36*, 1345–1346.
[9] H. Haller, S. Riedel, *Z. Anorg. Allg. Chem.* **2014**, *640*, 1281–1291.
[10] a) S. Riedel, T. Köchner, X. Wang, L. Andrews, *Inorg. Chem.* **2010**, *49*, 7156–7164; b) T. Vent-Schmidt, F. Brosi, J. Metzger, T. Schlöder, X. Wang, L. Andrews, C. Müller, H. Beckers, S. Riedel, *Angew. Chem. Int. Ed.* **2015**, *54*, 8279–8283, *Angew. Chem.* **2015**, *127*, 8397.
[11] a) M. P. Bogaard, J. Peterson, A. D. Rae, *Acta Crystallogr. Sect. B* **1981**, *37*, 1357–1359; b) J. Taraba, Z. Zak, *Inorg. Chem.* **2003**, *42*, 3591–3594.
[12] K. Sonnenberg, P. Pröhm, N. Schwarze, C. Müller, H. Beckers, S. Riedel, *Angew. Chem. Int. Ed.* **2018**, *57*, 9136–9140, *Angew. Chem.* **2018**, *130*, 9274.
[13] R. Brückner, P. Pröhm, A. Wiesner, S. Steinhauer, C. Müller, S. Riedel, *Angew. Chem. Int. Ed.* **2016**, *55*, 10904–10908, *Angew. Chem.* **2016**, *128*, 11064.
[14] R. Brückner, H. Haller, S. Steinhauer, C. Müller, S. Riedel, *Angew. Chem. Int. Ed.* **2015**, *54*, 15579–15583, *Angew. Chem.* **2015**, *127*, 15800.
[15] a) G. Cavallo, P. Metrangolo, R. Milani, T. Pilati, A. Priimägi, G. Resnati, G. Terraneo, *Chem. Rev.* **2016**, *116*, 2478–2601; b) T. Clark, M. Hennemann, J. S. Murray, P. Politzer, *J. Mol. Model.* **2007**, *13*, 291–296.
[16] H. Keil, K. Sonnenberg, C. Müller, R. Herbst-Irmer, H. Beckers, S. Riedel, D. Stalke, *Angew. Chem. Int. Ed.* **2021**, *60*, 2569–2573, *Angew. Chem.* **2021**, *133*, 2600–2604 .
[17] B. M. Powell, K. M. Heal, B. H. Torrie, *Mol. Phys.* **1984**, *53*, 929–939.
[18] B. Schmidt, S. Ponath, J. Hannemann, P. Voßnacker, K. Sonnenberg, M. Christmann, S. Riedel, *Chem. Eur. J.* **2020**, *26*, 15183–15189.
[19] H. Haller, M. Ellwanger, A. Higelin, S. Riedel, *Z. Anorg. Allg. Chem.* **2012**, *638*, 553–558.
[20] A. Bondi, *J. Phys. Chem.* **1964**, *68*, 441–451.
[21] T. Bernstein, F. H. Herbstein, *Acta Crystallogr.* **1968**, *B24*, 1640–1645.
[22] K.-F. Tebbe, R. Buchem, *Z. Kristallogr. Cryst. Mater.* **1995**, *210*, 438–441.
[23] K.-F. Tebbe, R. Buchem, *Z. Kristallogr. Cryst. Mater.* **1996**, *211*, 689–694.
[24] A. N. Nesmeyanov, L. P. Yur'eva, R. B. Materikova, B. Y. Getnarski, *Russ. Chem. Bull.* **1965**, *14*, 711–713.
[25] a) S. Zürcher, J. Petrig, V. Gramlich, M. Wörle, C. Mensing, D. von Arx, A. Togni, *Organometallics* **1999**, *18*, 3679–3689; b) J. Pickardt, H. Schumann, R. Mohtachemi, *Acta Crystallogr.* **1990**, *C46*, 39–41.
[26] a) M. Malischewski, M. Adelhardt, J. Sutter, K. Meyer, K. Seppelt, *Science* **2016**, *353*, 678–682; b) M. Malischewski, K. Seppelt, J. Sutter, F. W. Heinemann, B. Dittrich, K. Meyer, *Angew. Chem. Int. Ed.* **2017**, *56*, 13372–13376, *Angew. Chem.* **2017**, *129*, 13557–13561; c) M. Malischewski, K. Seppelt, J. Sutter, D. Munz, K. Meyer, *Angew. Chem. Int. Ed.* **2018**, *57*, 14597–14601, *Angew. Chem.* **2018**,*130*,14806–14810.
[27] A. W. Addison, T. N. Rao, J. Reedijk, J. van Rijn, G. C. Verschoor, *J. Chem. Soc. Dalton Trans.* **1984**, 1349–1356.
[28] V. Štrukil, E. Lekšić, E. Meštrović, M. Eckert-Maksić, *Aust. J. Chem.* **2014**, *67*, 1129–1133.
[29] G. M. Sheldrick, *Acta Crystallogr.* **2008**, *A64*, 112–122.
[30] G. M. Sheldrick, *Acta Crystallogr.* **2015**, *C71*, 3–8.
[31] O. V. Dolomanov, L. J. Bourhis, R. J. Gildea, J. A. K. Howard, H. Puschmann, *J. Appl. Crystallogr.* **2009**, *42*, 339–341.
[32] A. Klamt, G. Schüürmann, *J. Chem. Soc. Perkin Trans. 2* **1993**, 799–805.
[33] TURBOMOLE GmbH, *TURBOMOLE V7.3*: a development of University of Karlsruhe and Forschungszentrum Karlsruhe GmbH, **2018**.
[34] a) A. D. Becke, *J. Chem. Phys.* **1993**, *98*, 5648–5652; b) C. Lee, W. Yang, R. G. Parr, *Phys. Rev. B* **1988**, *37*, 785–789; c) S. H. Vosko, L. Wilk, M. Nusair, *Can. J. Phys.* **1980**, *58*, 1200–1211; d) P. J. Stephens, F. J. Devlin, C. F. Chabalowski, M. J. Frisch, *J. Phys. Chem.* **1994**, *98*, 11623–11627; e) S. Grimme, J. Antony, S. Ehrlich, H. Krieg, *J. Chem. Phys.* **2010**, *132*, 154104; f) A. D. Becke, E. R. Johnson, *J. Chem. Phys.* **2005**, *123*, 154101; g) E. R. Johnson, A. D. Becke, *J. Chem. Phys.* **2005**, *123*, 24101; h) E. R. Johnson, A. D. Becke, *J. Chem. Phys.* **2006**, *124*, 174104.
[35] S. Grimme, *J. Chem. Phys.* **2003**, *118*, 9095–9102.
[36] F. Weigend, R. Ahlrichs, *Phys. Chem. Chem. Phys.* **2005**, *7*, 3297–3305.
[37] M. J. Turner, J. J. McKinnon, S. K. Wolff, D. J. Grimwood, P. R. Spackman, D. Jayatilaka, M. A. Spackman, *CrystalExplorer17;* University of Western Australia, **2017**.

Manuscript received: November 25, 2020
Revised manuscript received: December 22, 2020
Accepted manuscript online: December 28, 2020